First Prize

MECHANICAL PROPERTIES OF THIN FILMS QUANTIFIED VIA INSTRUMENTED INDENTATION

K. J. Van Vliet and A. Gouldstone

Metallic coatings are primarily designed to enhance surface properties such as corrosion resistance, thermal protection, and tribological behaviour of a particular component in service. However, the deposition of such coatings inherently modifies the microstructure of the coating, resulting in mechanical properties of the coating that may differ significantly from those of the starting material from which the coating was produced. In addition, residual stresses are often present in the coating, and are strongly dependent upon deposition method and coating thickness. These stresses can lead to failure of the component owing to through-thickness cracking or interface delamination. Thus, it is clear that in order to maximise coating performance, the mechanical properties and stress state of the coating must be well characterised. Instrumented depth sensing indentation provides a means of quantifying the mechanical behaviour of the coated component on various size scales, depending on the maximum depth of the indentation. In addition, once mechanical properties have been ascertained via indentation, this method can also serve as a non-destructive quality control test during production. In the present work experimental and computational studies of micro- and nanoindentation on monolithic and coated metallic systems, including structural engineering alloys and microelectronic thin films, are described. The effects of material anisotropy, crystallographic orientation, and film thickness on the indentation response are considered, and these are correlated with the mechanical properties and residual stress state of the various systems. *SE/392*

The authors are in the Laboratory for Experimental and Computational Micromechanics, Massachusetts Institute of Technology, Cambridge, MA 02139, USA. *Contribution to the 2000 Bodycote International Paper Competition.*

INTRODUCTION

As engineering coatings and thin films continue to increase in structural complexity and industrial importance, the need for accurate assessment of the mechanical properties and residual stress state also increases. Instrumented indentation, a modification of the simple hardness test, is particularly well suited for such investigations. This method samples nano- to micrometre scale volumes of material. Thus, the mechanical behaviour of the coating material can be assessed independently of that of the underlying substrate. This method is based on continuum mechanics, and is thus equally applicable to indentations of nano-, micro-, and millimetre depths, but neglects microstructural length scales such as grain size.

In the present study, experimental and computational results for indentation of copper and aluminium thin films, coatings, and monoliths are presented. The goal of this work is to correlate experiments and theory in order to extract the mechanical properties of a given coating via indentation. By correlating experimental and computational results, it is shown that indentation can be a non-destructive, rapid, inexpensive procedure from which the full stress–strain response of a given thin film system is ascertained.

INSTRUMENTED INDENTATION

Short history

Instrumented indentation is a relatively new mechanical testing technique, derived from the crude hardness test. The hardness test is based on the basic correlation between the localised response of a material to an applied load and its overall resistance to permanent deformation, or yielding. In 1900, J. A. Brinell, a Swedish metallurgist at Fagersta Ironworks, invented this method in order to easily compare various heat treatments of steel.[1] The method is designed as follows: a small, hardened steel ball of known diameter D is pushed into a flat metal surface to a given load P. The area of the resulting impression is measured upon unloading, and the hardness of the material is calculated as

$$p_{\text{avg}} = \frac{P}{\pi r^2} \quad . \quad . \quad . \quad . \quad . \quad . \quad . \quad . \quad . \quad . \quad . \quad (1)$$

where p_{avg} is the hardness, or average pressure beneath the indenter, and r is the radius of the projected circular indentation.[2] In 1951, Tabor revived interest in the development of this technique. He suggested that determination of the average pressure via equation (2) at several different maximum applied loads would approximate the relationship between true flow stress and strain.[3] Assuming the material exhibited no strain hardening, Tabor related the indentation parameters to the material's mechanical properties as

$$\sigma = p_{\text{avg}}/3 \quad . \quad . \quad . \quad . \quad . \quad . \quad . \quad . \quad . \quad . \quad . \quad (2)$$

$$\varepsilon = 0{\cdot}2(d/D) \quad . \quad . \quad . \quad . \quad . \quad . \quad . \quad . \quad . \quad . \quad . \quad (3)$$

where σ is the true flow stress, ε is the true plastic strain, d is the indentation diameter, and D is the indenter diameter. In this way, Tabor proposed the

 ISSN 0267–0844

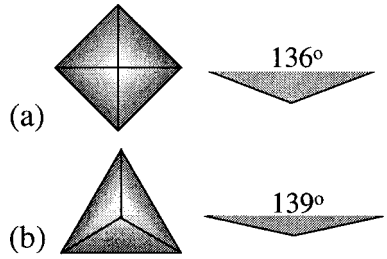

a Vickers indenter; *b* Berkovich indenter

1 *Sharp indenter geometries*

construction of stepwise stress–strain curves from spherical indentation.

In the early 1980s, the microelectronics industry prompted modification of this method. Miniaturisation of circuit components, including the incorporation of thin films, precluded the use of traditional mechanical testing methods such as simple tension. Thus, individual research groups sought to capitalise on Tabor's promise of small scale mechanical testing.[4–6] However, instead of conducting a series of tests at various maximum loads, researchers created depth sensing indentation that would continuously record the increase in load and depth during a single test. Thus, in theory, a continuous stress–strain curve could be produced from a single indentation test. Currently, machines that can measure microNewton loads and nanometre depths are commercially available. Sharp indenters, such as the square or triangle based pyramid, as shown in Fig. 1, are preferred for thin film investigations because these indenters induce plasticity at shallow indentation depths.

Indentation analysis

A schematic illustration of the experimental sharp indentation response is shown in Fig. 2. During continuous loading, the load increases parabolically with depth

$$P = Ch^2 \qquad (4)$$

where h is the indentation depth. The severity of this parabola is quantified by the loading curvature C, which is a function of both the elastic and plastic properties of the indented material

$$C = M_1\sigma_{cr}\left(1+\frac{\sigma_y}{\sigma_{cr}}\right)\left(-M_2+\ln\frac{\sigma_y}{E^*}\right) \qquad (5)$$

where σ_{cr} is the stress at a level of critical plastic strain, σ_y is the yield stress, E^* is the elastic modulus of the material, and M_1 and M_2 are geometrical constants related to the shape of the sharp indenter.[7] Upon unloading from the maximum depth h_{max} and maximum load P_{max}, the initial change in load and depth dP/dh is owing to the elastic stiffness of the indented material

$$\frac{dP}{dh} = \frac{E^*}{\beta(A_{max})^{1/2}} \qquad (6)$$

where A_{max} is the maximum projected area of indentation and β is a geometrical constant related to the shape of the indenter. The determination of A_{max} is not trivial owing to both experimental and material complications. Obviously, this quantity cannot be measured directly because the maximum contact area is achieved when the material is fully loaded; any elastic recovery of this indentation upon unloading will change the measured area. In addition, real materials, which strain harden, tend to pileup and sink in around the indenter perimeter, distorting the contact area. For these reasons, correlations between the normalised plastic work of indentation W_p/W_t, shown in Fig. 2 and the true A_{max} have been derived through three-dimensional finite element modelling (FEM).[7] Owing to the normalisation of all quantities given in Table 1 for a critical plastic strain of 29%, these relationships are true for all materials.

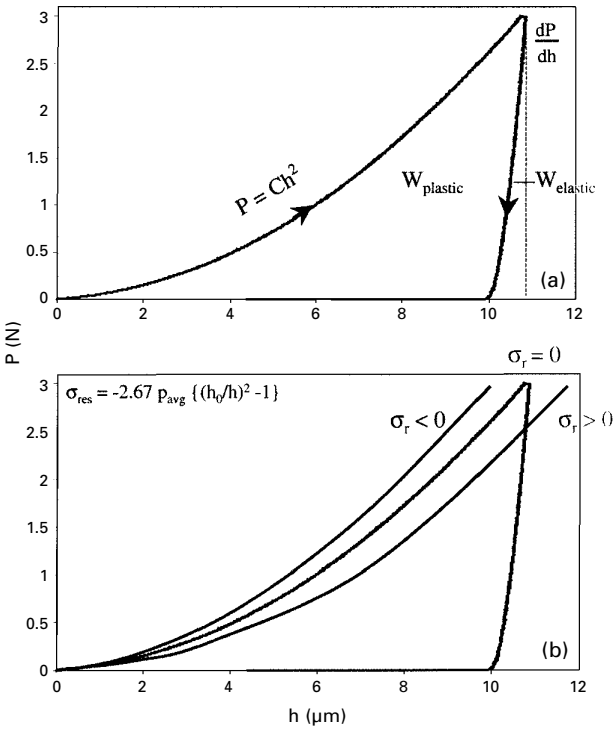

2 ***a*** *sharp indentation response and relevant curve parameters;* ***b*** *effect of residual stress on indentation response*

Using equations (4)–(6) in conjunction with the values given in Table 1, the elastic and plastic mechanical properties of the indented material can be calculated through a simple analysis of the indentation response. In addition, the residual stress state of a material can be calculated through comparison of the indentation response before and after residual stress has been induced. Figure 2*b* illustrates the effect of both compressive and tensile residual stress on the indentation response of a material. Naturally, if the indented material is in a

Table 1 Numerically determined correlations between material strain hardening, residual impression depth, and maximum contact area (Ref. 8)

$(\sigma_{cr}-\sigma_y)/\varepsilon_{cr}E^*$	W_p/W_t	A_{max}/h^2
1·00	0·00	9·82
0·33	0·76	16·00
0·27	0·875	24·50
0·05	0·91	25·50
0·025	0·94	28·99
0·00	1·00	43·35

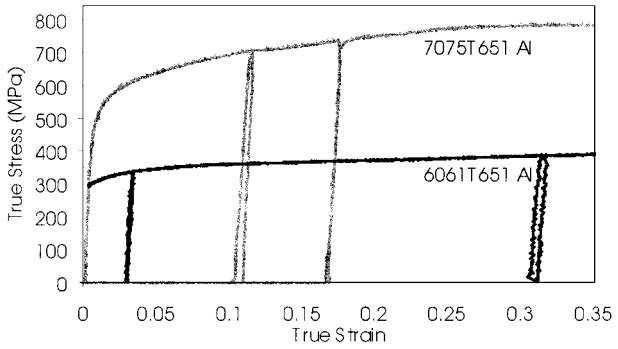

3 *Simple compression stress–strain response for two bulk Al alloys*

state of residual compressive stress, the indenter will penetrate the material less deeply for a given applied load. The difference between these maximum depths allows for the calculation of the residual stress magnitude

$$\sigma_{res} = M_3 p_{avg}(h/h_0)^2 \quad . \quad . \quad . \quad . \quad . \quad . \quad . \quad . \quad (7)$$

where h and h_0 are the maximum depths with and without residual stress, respectively, and M_3 is a geometric constant related to the indenter shape.[8]

In the following sections, these claims will be validated through results from monolithic materials, and then extended to coatings and thin films.

VALIDATION OF METHOD FOR BULK MATERIALS

Two industrially relevant aluminium alloys were chosen to study the indentation response of bulk materials: 7075T651 and 6061T651. The uniaxial compressive stress–strain response of both alloys was assessed in order to compare their mechanical properties with those calculated from the indentation response, as shown in Fig. 3. Clearly, both alloys exhibit the same elastic modulus, but 7075T651 possesses a higher yield stress and greater degree of strain hardening.

The microindentation response (indentation to micrometre scale depths) of both alloys is shown in Fig. 4. The 7075T651 shows a stiffer plastic response, as is manifest in the greater loading curvature C. This response results in a smaller indentation area A_{max} for the same maximum load, suggesting the material is more resistant to plastic deformation. This

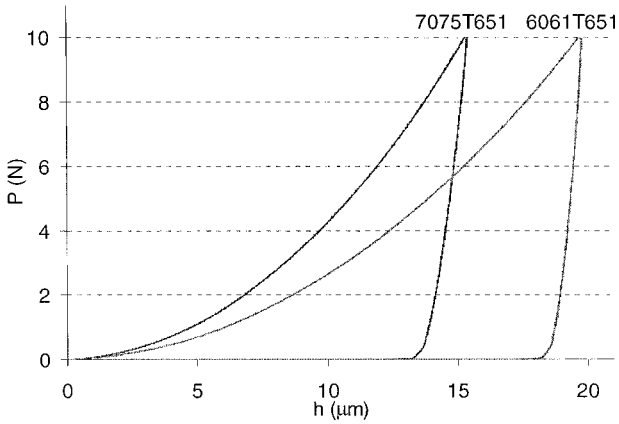

4 *Experimental indentation response for two bulk aluminium alloys: note that plastically stiffer alloy shows greater yield stress and strain hardening in simple compression*

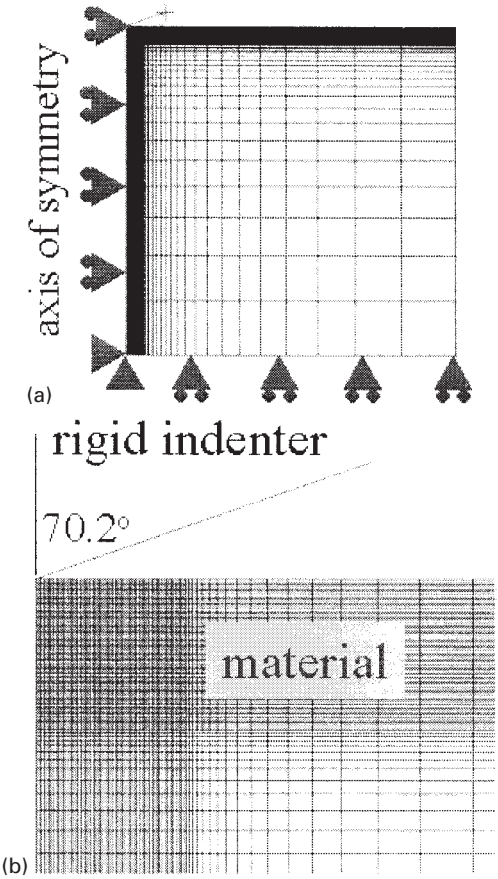

a whole field; *b* close up of initial contact region.

5 *Two-dimensional axisymmetric finite element mesh used in indentation simulation of bulk materials*

qualitative analysis is substantiated by the simple compression results shown in Fig. 3. These indentation results were confirmed through experiments at a series of maximum loads to ensure that continuum mechanics were valid for these materials at the maximum loads.

Using the simple compression data as material input for finite element calculations, indentation was simulated using a two-dimensional axisymmetric FEM constructed using the commercially available ABAQUS 5·8 software package. This mesh and its boundary conditions are shown in Fig. 5. As is clear from Fig. 6, the predicted indentation response resulting from the assumption of these mechanical properties agrees extremely well with the experimental indentation response. This correspondence validates the use of instrumented indentation in the quantification of mechanical properties of indented materials. If the predicted indentation, which assumes only the mechanical properties derived from simple compression of a material, matches the experimental indentation of that same material, the mechanical properties of a given material can be calculated directly from the experimental indentation response.

THIN FILMS AND COATINGS

Aluminium coatings

The natural extension of this work is to consider whether the mechanical properties of a coating can be unambiguously determined from its indentation response. This analysis may be complicated by the presence of an underlying substrate with its own

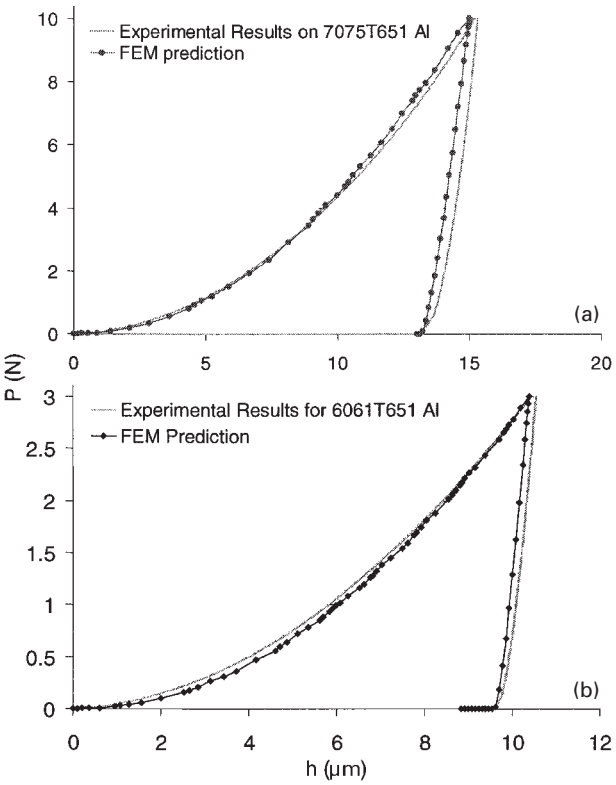

6 *Comparison of experimental and FEM indentation response for* ***a*** *7075T651 and* ***b*** *6061T651 Al alloys*

unique set of mechanical properties. Thus, one important issue is the maximum depth of indentation to which a coating can be indented before the substrate affects the indentation response.

To analyse this issue, sharp indentation of an Al coating on a perfectly elastic alumina substrate was modelled, using essentially the same mesh and boundary conditions as discussed above (Fig. 5). FEM has no inherent length scale; that is, although the coating was modelled to be one-fortieth the thickness of the substrate, its absolute thickness was not designated. As shown in Fig. 7, the loading curvature C of the indentation response is indeed affected by the underlying substrate for indentation depths greater than 10% of the film thickness. In contrast, other parameters of the indentation curve such as dP/dh are much less affected by the substrate. As a result, the mechanical properties of the coating can only be unambiguously determined for very shallow indentation depths. This result needs to be generalised so that it is independent of film and substrate mechanical properties.

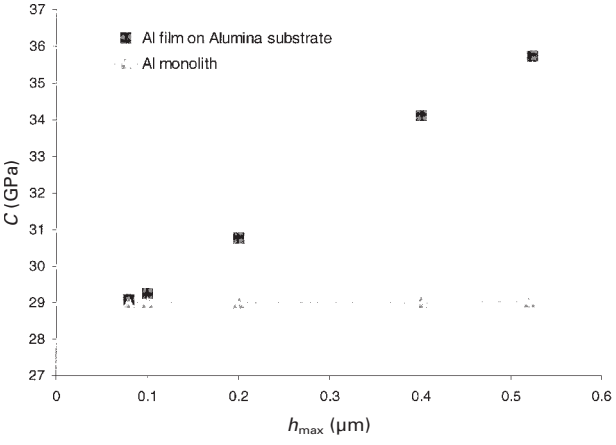

7 *FEM results comparing indentation response of monolithic Al and Al coating on alumina substrate: note that loading curvature increases from monolithic value at less than 10% film thickness*

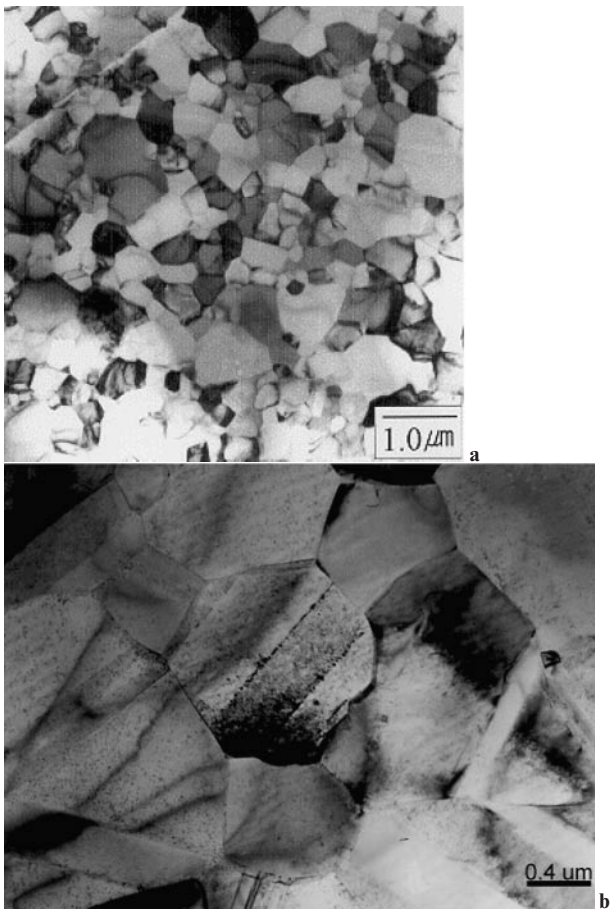

8 *TEM images of* ***a*** *polycrystalline Al film and* ***b*** *polycrystalline Cu film: film thickness 1 mm*

Single crystal aluminium thin films

Single crystal thin films of Al were prepared with varying crystallographic orientations: (110), (111), and (133). In addition, polycrystalline thin films of Al were prepared with varying thickness (0·3–1·0 μm) and grain size, and a predominantly (111) orientation normal to the substrate. The substrates used in all the specimens were (100) oriented, oxidised Si. A detailed account of the specimen preparation is given

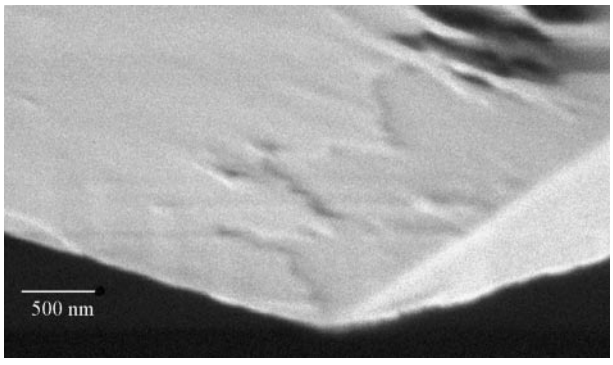

9 *Scanning electron micrograph of indenter tip used in experiments*

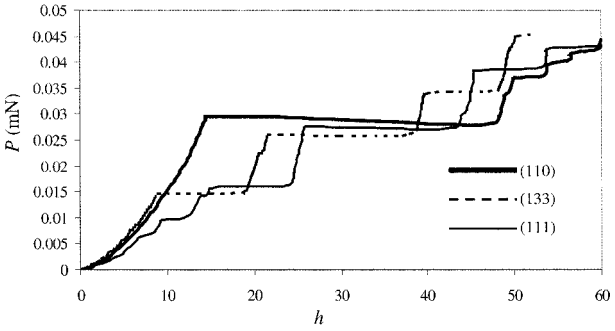

10 *Experimental nanoindentation response for single crystal Al thin films on Si substrates*

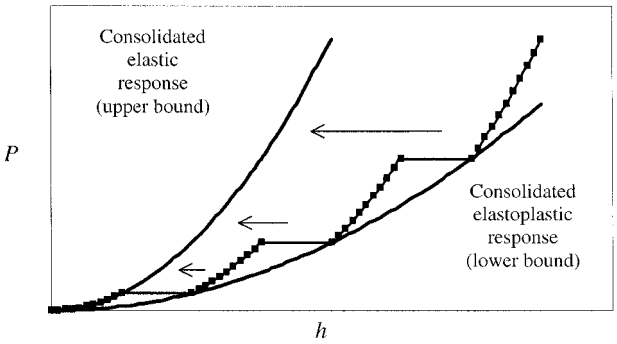

12 *Schematic graph of elastic upper bound and elastoplastic lower bound for P–h response*

in a previous paper.[9] Sample TEM images of the polycrystalline thin films are given in Fig. 8*a* and *b*. In both cases, the grain size is comparable to the thickness of the films.

Nanoindentation experiments on polycrystalline Al films were performed using a commercial nanoindenter. This diamond Berkovich indenter, although nominally sharp, had a finite tip radius R of 40–50 nm, as shown in Fig. 9. Nanoindentation experiments were conducted to a maximum load of $P = 0{\cdot}1$ mN, held at maximum load for 20 s, and then held for another 20 s at 90% of unloading, so as to correct for any thermal drift in the system. The indentations were examined using a commercial atomic force microscope. In order to neglect the effects of the substrate in this analysis, only loading curves to maximum depths less than 10% of the film thickness were considered.

Figure 10 shows loading curves for the three orientations of the Al single crystal films. The initial portions of the curves are parabolic, the curvatures of which are consistent with a sharp Berkovich indenter contacting an elastic material with a modulus of roughly 70 GPa.[10] Owing to the low degree of elastic anisotropy in Al, this elastic response does not vary much with crystallographic orientation. At some load P, the indenter sinks into the material with no increase in load. After this displacement 'burst', the indenter resumes elastic indentation, with subsequent bursts and elastic loading portions. In the literature, these bursts have been attributed to the nucleation and motion of dislocations underneath the indenter. Underneath a rounded indenter tip of radius R, the maximum shear stress τ_{max} in the material is a function of the load P.[11] This and other results reported in the literature on single crystal Au and Fe–Si have shown that this load P is that at which τ_{max} under the indenter reaches the critical shear strength of the material, in order to nucleate a dislocation in an otherwise perfect crystal.[12] Thus, the response under an indenter at such loads is characterised by discrete regions of elasticity and plasticity.

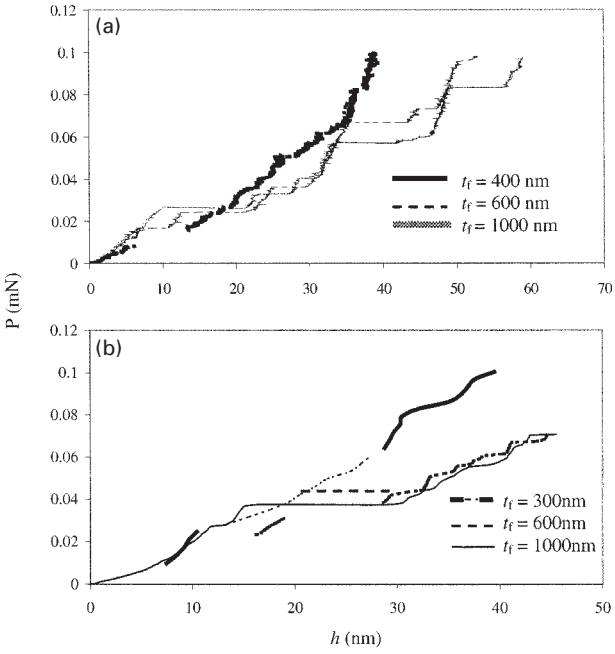

11 *Experimental nanoindentation response of polycrystalline* ***a*** *Al and* ***b*** *Cu films*

Polycrystalline aluminium and copper thin films

Figure 11*a* and *b* shows loading curves for polycrystalline Al and Cu thin films, respectively. Note that the initial elastic parabola is followed by displacement bursts. Also note that the response of the polycrystalline films is not as 'clean' as their single crystal counterparts, i.e. elastic loading ceases at lower loads, and the bursts are not as pronounced. This difference between the single and polycrystalline response may be attributed to the existence of grain boundaries. Grain boundaries may provide defects in the region of the indenter, which could move and subsequently cause inelastic deformation at stresses well below the critical shear strength of the material. However, as in the case of the single crystal films, it is shown that elastic and plastic deformation are discretely separated at such indentation loads.

One other important feature of the curves for the polycrystalline films is the dependence of the loading curvature on film thickness. Consider the graph in Fig. 12. A typical low load P–h curve can be described in the following manner: if the bursts were removed, the response would be purely elastic. This represents an upper bound stiffness for the material, whether thin film or bulk. If, however, the displacement bursts are considered, a lower bound can also be constructed by connecting the rightmost points of the bursts. This bound represents both the elastic and plastic deformation in the material. The construction of such a lower bound for the indentation responses in Fig. 11 shows that the curvature of these elastoplastic bounds C increases as film thickness decreases. This is consistent with results from widespread investigations in the literature on the strength of thin films, which report

that film strength increases with decreasing film thickness.[13–18] Such an observation can be rationalised by postulating that dislocations emitted from underneath the indenter are slowed or otherwise hindered as they near the film/substrate interface. For thinner films, this hindrance would ostensibly occur at shallower depths, causing the greater observed curvature C in the elastoplastic bounds.

CONCLUSIONS

Through experiment and computation, it has been shown that the mechanical properties of a coating can be quantified through instrumented indentation. In addition, FEM has revealed that the underlying substrate may affect the indentation response if the indentation depth is greater than 10% of the coating thickness. Finally, experiments at very shallow indentation depths have indicated that indentation of both single crystal and polycrystalline thin films can elucidate mechanical behaviour unique to these systems, such as a yield stress that is inversely proportional to the film thickness, as well as instances of discrete plasticity at very high stresses.

ACKNOWLEDGEMENTS

The authors would like to acknowledge their advisor, Professor Subra Suresh, for his encouragement and inspiration, as well as B. W. Choi at Lawrence Livermore National Laboratories where much of the experimental work was conducted, and M. Dao for his FEM expertise. One of the authors (KJVV) is funded by the National Defence Science and Engineering Graduate Fellowship, and the other author (AG) is funded by MARCO Focused Research Center on Interconnects.

REFERENCES

1. 'Brinell, Johan August', 1999–2000, www.Britannica.com.
2. E. Z. MEYER: *Ver. Deut. Ing.*, 1908, **52**, 645–654.
3. D. TABOR: 'The hardness of metals,' 67–76; 1951, New York, NY, Oxford University Press.
4. M. NISHIBORI and K. KINOSITA: *Thin Solid Films*, 1978, **48**, 325–331.
5. J. PETHICA, R. HUTCHINGS, and W. C. OLIVER: *Philos. Mag.*, 1983, **A48**, 593–606.
6. J. L. LOUBET, J. M. GEORGES, J. M. MARCHESINI, and G. MEILLE: *J. Tribol.*, 1984, **106**, 43–48.
7. S. SURESH and A. E. GIANNAKOPOULOS: *Acta Mater.*, 1998, **46**, 5755.
8. A. E. GIANNAKOPOULOS and S. SURESH: *Acta Mater.*, 1999, **48**, 5000.
9. A. GOULDSTONE, H.-J. KOH, K.-Y. ZENG, A. E. GIANNAKOPOULOS, and S. SURESH: *Acta Mater.*, 2000, **46**, 2277.
10. P.-L. LARSSON, A. E. GIANNAKOPOULOS, E. SODERLUND, D. J. ROWCLIFFE, and R. VESTERGAARD: *Int. J. Solids Struct.*, 1996, **33**, 221.
11. K. L. JOHNSON: 'Contact mechanics'; 1985, Cambridge, Cambridge University Press.
12. W. W. GERBERICH, J. C. NELSON, E. T. LILLEODDEN, P. ANDERSON, and J. T. WYROBEK: *Acta Mater.*, 1996, **44**, 3585.
13. R. VENKATRAMAN, J. C. BRAVMAN, W. D. NIX, P. W. DAVIES, P. A. FLINN, and D. B. J. FRASER: *Electron. Mater.*, 1990, **10**, 1231.
14. M. KOBRINSKY and C. V. THOMPSON: *Acta Mater.*, 2000, **48**, 625.
15. E. CHU, Y.-L. SHEN, and S. SURESH: Lexcom Report, Massachusetts Institute of Technology, Cambridge, MA, 1996.
16. R.-M. KELLER, S. P. BAKER, and E. ARZT: *J. Mater. Res.*, 1998, **13**, 1307.
17. P. R. BESSER: 'X-ray determination of thermal strains and stresses in thin aluminum films and line', PhD dissertation, Stanford University, 1993.
18. P. A. FLINN: *J. Mater. Res.*, 1991, **6**, 1498.